



The surface and bulk oxidation of zirconium
by Brian Paul Thiesen

A thesis submitted in partial fulfillment of the requirements for the degree of Master of Science in
Chemical Engineering
Montana State University
© Copyright by Brian Paul Thiesen (1988)

Abstract:

The oxidation of zirconium at high temperatures involves both the formation of a surface oxide, and absorption of oxygen into the bulk Zr. The hcp lattice of Zr is reported to absorb up to 29.8 at. % oxygen, which occupies the interstitial sites. The simultaneous surface oxidation and diffusion of oxygen into the bulk Zr were observed at temperatures of 1073, 1173 and 1243 K. Experimental results were compared to predicted results from a model developed here to evaluate values of the oxidation kinetic parameters. Samples of Zr, 0.025 cm thick, were saturated with oxygen by soaking surface-oxidized samples in an argon atmosphere at 1243 K. The initial surface oxidation properties of saturated Zr were compared to pure Zr by AES-analysis.

The model of the oxidation process assumes that diffusion of O_2 through the oxide layer is rate limiting. The oxide growth at the oxide Zr interface is described by a mass balance. The principle parameter in the model is the product, D/δ , the diffusion coefficient of oxygen in ZrO_2 and the oxygen concentration difference across the oxide. The model was calibrated by two completely separate methods. The first compared model predicted curves of mass vs. time to those produced experimentally. The second method compared predicted oxide thicknesses at specific times and temperatures with those observed experimentally. A value for δ from the literature was assumed. Then D as a function of temperature was determined for both experimental methods. From the mass gain curve fitting method the diffusion coefficient, $D = 1.6 \times 10^{-5} \exp(-20700/RT)$ was found. From the oxide thickness comparison the diffusion coefficient, $D = 2.0 \times 10^{-2} \exp(-34300/RT)$ was found. It is concluded that the primary oxygen diffusion path is along grain boundaries, and that D is a function of extent of oxidation due to changing oxide crystal size during oxidation.

Saturated and pure Zr samples were exposed to successive exposures of O_2 at room temperature, interrupted by sequential AES analysis. Results of the AES study indicate that Zr:Oss surface oxidation is essentially the same as that of pure Zr. The oxygen concentration of sputter-cleaned Zr:Oss was estimated to be 28.8 at. % oxygen by quantitative AES analysis.

THE SURFACE AND BULK OXIDATION OF ZIRCONIUM

by

Brian Paul Thiesen

A thesis submitted in partial fulfillment
of the requirements for the degree

of

Master of Science

in

Chemical Engineering

MONTANA STATE UNIVERSITY
Bozeman, Montana

March 1988

N378
T3475

APPROVAL

of a thesis submitted by

Brian Paul Thiesen

This thesis has been read by each member of the thesis committee and has been found to be satisfactory regarding content, English usage, format, citations, bibliographic style, and consistency, and is ready for submission to the College of Graduate Studies.

April 6, 88
Date

Max C. Deiber
Chairperson, Graduate Committee

Approved for the Major Department

April 7, 88
Date

John T. Sears
Head, Major Department

Approved for the College of Graduate Studies

4-14-88
Date

Ms Malone
Graduate Dean

STATEMENT OF PERMISSION TO USE

In presenting this thesis in partial fulfillment of the requirements for a master's degree at Montana State University, I agree that the Library shall make it available to borrowers under rules of the Library. Brief quotations from this thesis are allowable without special permission, provided that accurate acknowledgment of source is made.

Permission for extensive quotation from or reproduction of this thesis may be granted by my major professor, or in his absence, by the Dean of Libraries when, in the opinion of either, the proposed use of the material is for scholarly purposes. Any copying or use of the material in this thesis for financial gain shall not be allowed without my written permission.

Signature

Date

4-13-88

ACKNOWLEDGMENTS

The author wishes to thank the faculty and staff of the Chemical Engineering Department at Montana State University for their guidance and assistance.

Special thanks to Dr. M. Deibert for his advice and support throughout the course of this research and thesis preparation.

The author also wishes to thank Dr. Frank P. McCandless and Dr. Robert L. Nickelson for the use of their equipment and assistance.

TABLE OF CONTENTS

	Page
APPROVAL.....	ii
STATEMENT OF PERMISSION TO USE.....	iii
ACKNOWLEDGMENTS.....	iv
TABLE OF CONTENTS.....	v
LIST OF TABLES.....	viii
LIST OF FIGURES.....	ix
ABSTRACT.....	xii
INTRODUCTION.....	1
Background.....	1
Related Research.....	3
General Characteristics.....	4
Effect of Oxygen Pressure on the Oxidation of Zr	8
Effect of the Oxidizing Agent.....	8
Diffusion Characteristics.....	9
Surface Science.....	11
RESEARCH OBJECTIVES.....	13
MODEL DEVELOPMENT.....	14
Mechanisms During Surface Oxidation of Zr.....	14
Ionic Transport in the Oxide.....	16
Electron Transport in the Oxide.....	19
Migration of Oxygen Through the Oxide.....	20
Development of a Mathematical Model.....	20
Adsorption.....	21
Mass Flux Across the Oxide.....	21
Diffusion of Oxygen into the Bulk Zr.....	22
Interface.....	23
Boundary Conditions.....	26

TABLE OF CONTENTS-Continued

	Page
EXPERIMENTAL EQUIPMENT.....	32
Reactor for Oxidation and Saturation of Zr.....	32
Surface Spectroscopy Methods.....	34
Scanning Electron Microscopy.....	34
Auger Electron Spectroscopy.....	35
EXPERIMENTAL PROCEDURES.....	37
Oxidation and Saturation Procedures.....	37
Sample Preparation.....	37
Experimental Equipment and Procedure.....	38
Determination of Time to Saturate Samples.....	40
AES Analysis Procedure.....	41
SEM Analysis Procedure.....	43
RESULTS AND DISCUSSION.....	45
Analysis of Saturated Zirconium.....	45
AES Spectra Analysis by Seah Method.....	46
Depth Profile.....	49
Initial Oxidation at Room Temperature.....	51
Diffusion Coefficient Determination.....	54
Model Application.....	55
Isothermal Model Correlations from	
Curve Fitting Method.....	58
Evaluation of $D_{\sigma}\delta C_{\sigma}$ from Curve Fitting.....	60
Experimental Error Involved with Curve Fitting..	64
Isothermal Model Correlations with	
Oxide Thickness Measurements.....	67
Evaluation of $D_{\sigma}\delta C_{\sigma}$ from Experimental	
Oxide Thicknesses.....	69
Experimental Error Involved with	
Oxide Thicknesses.....	69
Determination of D_{σ} as a Function of Temperature..	71
Deviations Between Experimental and	
Published Values of D_{σ}	74
Changing Characteristics of the Oxide.....	76
Effect of Warm-Up and Cool-Down.....	77
CONCLUSIONS.....	83
RECOMMENDATIONS FOR FUTURE RESEARCH.....	84
REFERENCES CITED.....	85

TABLE OF CONTENTS-Continued

	Page
APPENDIX.....	89
Computer Program: Temperature control in the reactor.....	90
Computer Program: Isothermal Model I.....	91
Computer Program: Non-isothermal Model II.....	95
Computer Program: Model III, Diffusion model to determine the time to reach 99.99% saturation at the midplane.	99

LIST OF TABLES

Table	Page
1. Variables used in the model.....	28
2. Exposure times and pressures utilized in Surface oxidation study.....	43
3. Predicted times to reach 99.99% saturation at midplane and actual time of run.....	45
4. AES primary peak intensities for pure and Zr:Oss.....	54
5. Oxidation conditions of each Zr sample.....	57
6. Percent of total time sample was in cool-down and warm-up stage, and the percent deviation of final mass between Cahn 29 and R-100 balances.....	58
7. $D_{\sigma} \delta C_{\sigma}$ from oxide thickness measurements and mass gain curve fitting.....	64
8. D_{σ} from oxide thickness measurements and mass gain curve fitting.....	74
9. Experimental oxide thicknesses and the percent deviation vs. predicted non-isothermal model oxide thicknesses.....	78

LIST OF FIGURES

Figure	Page
1. Partial phase diagram of the oxygen-zirconium system.....	5
2. A schematic representation of oxidation of Zr showing the four regions of oxidation rate.....	7
3. Schematic diagram of surface oxidation on Zr and the processes occurring in the oxide during oxidation.....	15
4. Mechanisms that occur in the surface oxide during the oxidation of Zr.....	17
5. Progression of the oxide-metal interface and the change in O concentration in bulk Zr at points C_n at time θ and points C'_n at time $\theta + \delta\theta$	25
6. Model predicted long term oxygen accumulation during surface oxidation of 0.025 cm thick Zr at 1243 K using a value of $D_O \delta C_O = -1.10 \times 10^{-10}$ mole O/cm sec. Accumulation of oxygen in bulk Zr and oxide layer shown separately.....	29
7. Model predicted surface and bulk oxidation of 0.025 cm thick Zr at 1243 K using a value of $D_O \delta C_O = -1.10 \times 10^{-10}$ mole O/cm sec. The progression of the oxide-metal interface and oxygen concentration are functions of time (in hours)....	30
8. Schematic of the oxidation and saturation system..	33
9. The AES spectrum from 78 eV to 178 eV for: (a) sputter cleaned pure Zr; (b) sputter cleaned Zr:Oss; (c) 10 L O_2 exposed Zr:Oss at room temperature; (d) 300 L O_2 exposed Zr:Oss at room temperature.....	47
10. Mole fraction of O and Zr in Zr:Oss as a function of sputter time.....	50
11. Mole fraction of O and Zr in pure and Zr:Oss as a function of oxygen exposure.....	53

Figure	Page
12. Typical experimental mass gain curve showing the effect of evacuating the system at the start of the run, and returning the system to atmospheric pressure at the end of the run.....	59
13. Experimental and isothermal model mass gains at 1073 K.....	61
14. Experimental and isothermal model mass gains at 1173 K.....	62
15. Experimental and isothermal model mass gains at 1243 K.....	63
16. Experimental and published mass gains; dashed lines this research at (a) 1173 K and (b) 1073 K; solid lines published (c) K. Osthagen et. al. at 1073 K (32), (d) J. Leviton et. al. at 1073 K (6), (e) C.J. Rosa at 1123 K (33).....	66
17. SEM 200X enlargement of polished Zr edge showing surface oxide growth after 6.3 hours at 1173 K in medical grade O ₂	68
18. Experimental and published oxide thicknesses: (a) this research at 1243 K, (b) this research at 1173 K, (c) J.P. Pemsler at 1373 K (34), (d) this research at 1073 K, (e) C.J. Rosa at 1123 K (33)...	70
19. Various diffusion coefficients of O ₂ -in ZrO ₂ : (a) this research from mass gain curve fitting; (b) this research from oxide thickness measurements; (c) and (d) Rosa and Hagel below and above the transition temperature respectively (38); (e) Smith (39); (f) Keneshea and Douglass (15); (g) Madyski and Smeltzer in single crystal near stoichiometric ZrO ₂ (26).....	73
20. Experimental and theoretical mass gains at 1073 K. (a) experimental, (b) isothermal model, (c) non-isothermal model.....	79
21. SEM 200X enlargement of a fractured Zr edge showing surface oxide growth after 10.4 hours at 1173 K in medical grade O ₂	82

Figure	Page
22. Computer Program: Temperature Control in the reactor.....	90
23. Computer Program: Isothermal Model I	91
24. Computer Program: Non-Isothermal Model II	95
25. Computer Program: Model III, Diffusion model to determine the time to reach 99.99% saturation at the midplane.....	99

ABSTRACT

The oxidation of zirconium at high temperatures involves both the formation of a surface oxide and absorption of oxygen into the bulk Zr. The hcp lattice of Zr is reported to absorb up to 29.8 at. % oxygen, which occupies the interstitial sites. The simultaneous surface oxidation and diffusion of oxygen into the bulk Zr were observed at temperatures of 1073, 1173 and 1243 K. Experimental results were compared to predicted results from a model developed here to evaluate values of the oxidation kinetic parameters. Samples of Zr, 0.025 cm thick, were saturated with oxygen by soaking surface-oxidized samples in an argon atmosphere at 1243 K. The initial surface oxidation properties of saturated Zr were compared to pure Zr by AES analysis.

The model of the oxidation process assumes that diffusion of O_2 through the oxide layer is rate limiting. The oxide growth at the oxide Zr interface is described by a mass balance. The principle parameter in the model is the product, $D_o \delta C_o$, the diffusion coefficient of oxygen in ZrO_2 and the oxygen concentration difference across the oxide. The model was calibrated by two completely separate methods. The first compared model predicted curves of mass vs. time to those produced experimentally. The second method compared predicted oxide thicknesses at specific times and temperatures with those observed experimentally. A value for δC_o from the literature was assumed. Then D_o as a function of temperature was determined for both experimental methods. From the mass gain curve fitting method the diffusion coefficient, $D_o = 1.6 \times 10^{-5} \text{EXP}(-20700/RT)$ was found. From the oxide thickness comparison the diffusion coefficient, $D_o = 2.0 \times 10^{-2} \text{EXP}(-34300/RT)$ was found. It is concluded that the primary oxygen diffusion path is along grain boundaries, and that D_o is a function of extent of oxidation due to changing oxide crystal size during oxidation.

Saturated and pure Zr samples were exposed to successive exposures of O_2 at room temperature, interrupted by sequential AES analysis. Results of the AES study indicate that Zr:Oss surface oxidation is essentially the same as that of pure Zr. The oxygen concentration of sputter-cleaned Zr:Oss was estimated to be 28.8 at. % oxygen by quantitative AES analysis.

INTRODUCTION

Background

Zirconium, Zr, is an abundant metal. However, its use in industry has remained limited. The nuclear industry uses about 90% of the total Zr refined as cladding for fuel rods, and is the largest single industry interested in the properties of Zr. In fact, had it not been for the advent of the nuclear age, Zr would probably be no more than a desk-top curiosity for chemists and researchers. Despite the largely reduced cost, due to the nuclear industry, Zr has found very little use except for a limited amount in the electronics industry.

Zirconium oxide, ZrO_2 , has found extensive use. It is extremely heat and chemically resistant. Hydrofluoric and sulfuric acids are the only chemicals that attack the oxide with any significant effect. Because of these properties, ZrO_2 ceramic tiles can be found in many high temperature applications. The oxide is also an effective catalyst for the coal-gas liquification process, where carbon oxides and hydrogen are passed over ZrO_2 at elevated temperatures resulting in carbon chain formations.

The surface study of catalytic reactions on ZrO_2 present difficulties when certain surface selective spectroscopy methods are used. When the ZrO_2 surface is bombarded with any charged particulate (argon ions, electrons, and etc.), the surface will become charged and deflect the beam. A deflected beam results in interference with the spectroscopy method. To address this difficulty, it has been proposed that surface oxides developed on a Zr metal substrate be used to electrically ground the ZrO_2 study surface. However, heating of the oxide coated metal to catalytic reaction temperatures under ultra-high vacuums results in the oxide layer disappearing. This phenomenon results when the oxygen dissolves into the bulk Zr (1). The dissolution of the oxide surface can be avoided if the oxide layer is grown on an oxygen saturated sample of Zr, denoted as Zr:Oss. Upon further study of this phenomenon, it has been determined to be feasible and valuable to examine the oxide metal interface and learn more about the kinetics of the surface oxidation and the bulk oxygen diffusion process in Zr. The objectives of this study are to produce Zr:Oss samples and to analyze the reaction of oxygen on the surface of bulk Zr.

Related Research

Extensive research has been done on the oxidation of Zr. A majority of the work has been accomplished by researchers in the nuclear industry. They have limited much of their work to conditions achieved in reactors, and usually study Zr alloys. Other research has expanded the knowledge about Zr in conditions other than those in a reactor. Both Douglas (2) and Cox (3) have performed extensive literature surveys. Douglas has compiled a list of observed results regarding kinetics of oxidation and values for the oxidation rate constants. Cox has summarized the theories and mechanisms of the oxidation process. From their work and other publications, a large variation in observed oxidation rates is apparent, as well as a lack of understanding of the mechanisms occurring at the oxide-metal interface.

Many of the general chemical and physical properties of Zr are well known. When Zr is exposed to certain conditions, it is usually predictable how it will respond. On the other hand, it is not clear as to why or by what mechanisms it reacts. Important factors that effect the surface oxidation and the diffusion of oxygen into bulk Zr are temperature, pressure, oxidizing environment, and impurities.

General Characteristics

At room temperature in air, bulk samples of Zr develop a protective surface oxide. On a polished surface, this oxide is about 60 Å thick (4). The cohesive surface oxide blocks the transport of oxygen to the underlying Zr, protecting the metal from further oxidation.

A distinguishing characteristic that separates Zr from many other metals is its ability to form interstitial solid solutions with large amounts of dissolved oxygen. A phase diagram of the oxygen-zirconium system is shown in Figure 1 (5). Recent measurements on this system indicate that a saturated Zr-oxygen solution contains about 29.8 atomic percent oxygen (4).

When a sample of Zr is exposed to oxygen, air, or steam, at elevated temperatures, two processes take place. The oxide layer thickens as the oxide layer's protective abilities are reduced. Simultaneously, oxygen diffuses into the bulk metal. The diffusion process into the metal causes no phase changes when the temperature remains below the α - β transition temperature of 1135 K for pure Zr. Above this temperature, pure Zr exists in the β -phase. The α - β transition is a change in the lattice structure of the Zr from hcp to bcc. As oxygen diffuses into the bulk β -phase, the structure transforms into a stabilized α -phase before the oxygen concentration reaches saturation, as can be seen in the phase diagram.

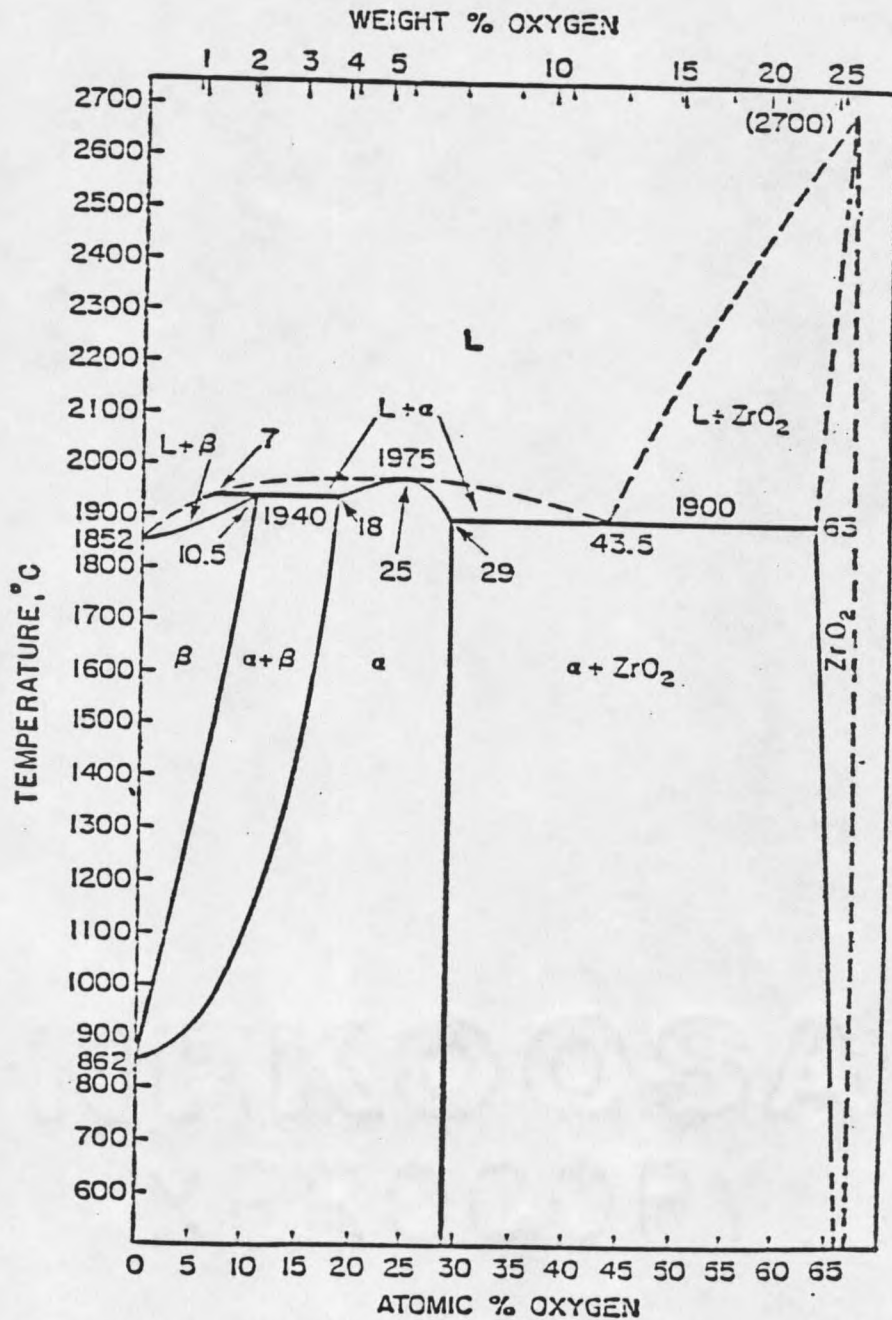


Figure 1. Partial phase diagram of the oxygen-zirconium system (5).

In measurements of the rates of mass gains of Zr at elevated temperatures in oxidizing environments, four regions of oxidation rates are observed (2,3,6). The transitions between the regions are recognized by the change in the rate of mass gain vs. time. A schematic of the transitions and the regions of oxidation are shown in Figure 2 as a plot of mass gain vs. time. The first two regions are observed primarily during low pressure and low temperature oxidation. These regions also occur at high pressures and temperatures, but too rapidly to be easily observed. The first reaction regime is characterized by an unpredictable initial oxidation rate. This region continues up to an oxygen mass gain range of 0 to .01 mg O/cm² of Zr surface. The second transition occurs at about .1 mg/cm², and is associated with a change between different types of second order kinetics. These short term changes in the oxidation rate are not generally noticeable when observing total oxidation extant above about 1 mg/cm². The third transition occurs at various degrees of oxidation, depending on the purity and pre-treatment of the sample.

The first transition is commonly associated with a change in the electrical conductivity of the surface oxide (2,8). The second is associated with the end of a period of amorphous oxide growth and its replacement with non-amorphous black surface oxide (3). The third transition is associated with a physical breakdown of the oxide from black to a white

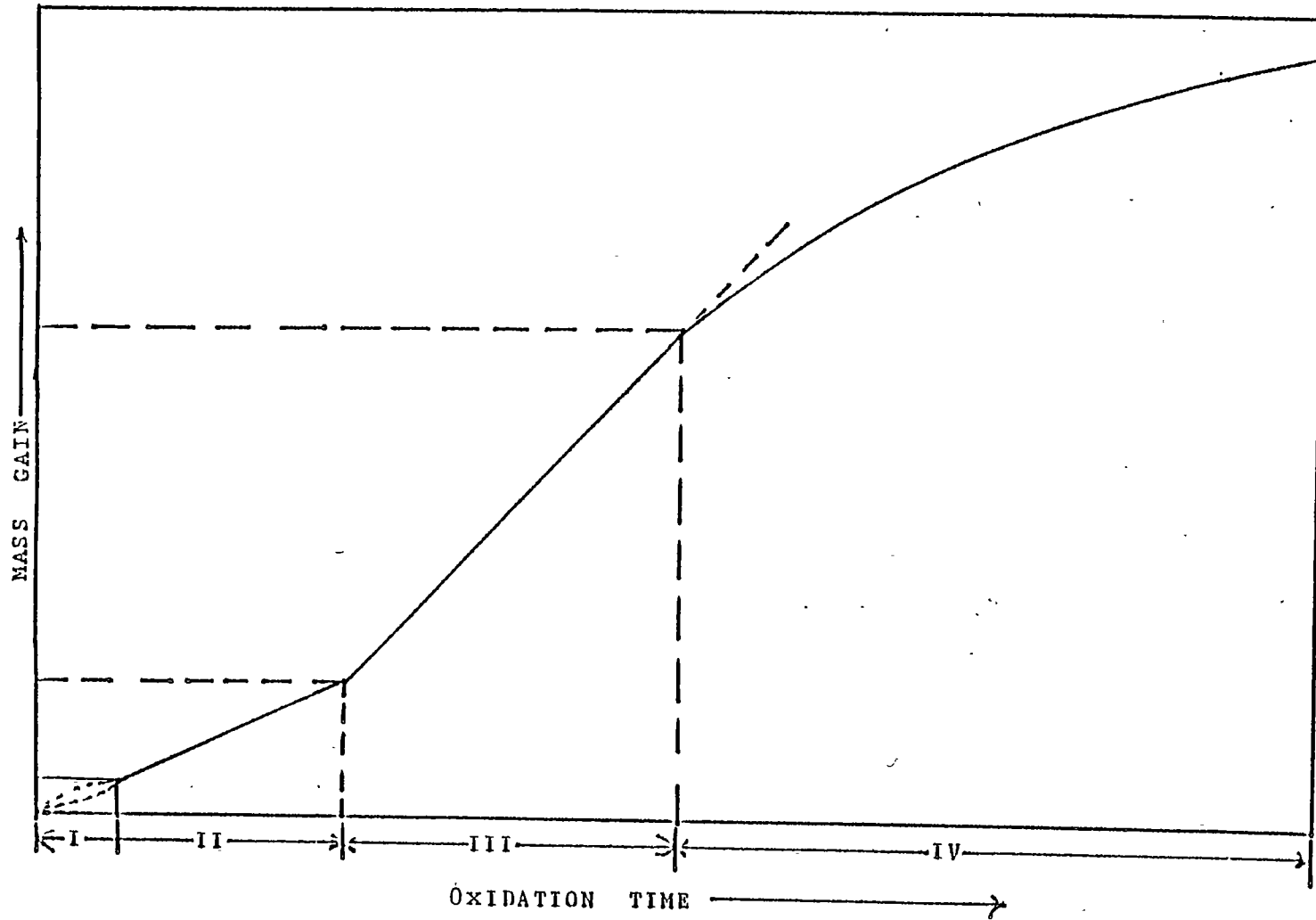


Figure 2. A schematic representation of oxidation of Zr showing the four regions of oxidation rate.

oxide together with flaking or spalling of the surface oxide. The extent of these oxidation regions depends upon the impurities in the Zr sample, as well as the temperature, pressure and oxidizing agent. Below is a description of the effect of each of these parameters on the rate of oxidation of Zr.

Effect of Oxygen Pressure on the Oxidation of Zr. The rate of diffusion of oxygen into Zr has been observed to be independent of O_2 pressure down to about 1 mm Hg (6,7). Below this pressure, the oxidation rate decreases until the pressure is sufficiently low that the oxide dissociates and dissolves into the bulk metal (1). This occurs when the concentration gradient across the oxide becomes sufficiently small that the transport of oxygen across the oxide is less than the rate of oxygen dissolution into the bulk Zr.

The Effect of the Oxidizing Agent. The oxidizing agent has some effect upon the initial rate of oxidation. The effect is only seen in the first two oxidation regions and doesn't significantly influence longer term oxidation. The unpredictability in the initial oxidation rate is believed to be related to the electrical conductivity of the oxidizing agent, the environment with the oxidizing agent and of the oxide layer (8).

Several investigations have shown that the method of surface preparation can strongly effect the initial

oxidation rate (2). This is believed to be due to a change in the conductivity, corresponding to a change in the surface chemical characteristics which are effected by pre-treatments of the surface. It has also been shown that small amounts of impurities may change the initial oxidation rate, probably from a change in the electrical conductivity of the surface oxide.

Diffusion Characteristics

There are many difficulties encountered in the study of the diffusion of oxygen into bulk Zr. Some methods of study have used indirect determination of oxygen content by measuring the microhardness, or the change in the lattice parameters, of the hexagonal close-packed structure (9-13). However, both of these methods are not accurate since neither microhardness nor the change in the hexagonal Zr lattice are directly proportional to the oxygen content in the bulk Zr (4). Direct methods of measurement have employed the etching away of incremented amounts of the surface, followed by the use of nuclear microanalysis to measure the oxygen content of the sequentially exposed surfaces (4). Literature values of the diffusion coefficient of oxygen in Zr are in good agreement with each other. A good average correlation, and the one used in the following analysis is $D_{\alpha} = 5.2 \exp(-50800/RT) \text{ cm}^2/\text{sec}$ (2).

Currently, published diffusion coefficients for oxygen in ZrO_2 are not in as good agreement as those in bulk Zr.

Several problems arise when attempting to evaluate this diffusion coefficient. One complication is associated with the determination of the oxygen concentration gradient through the oxide. Another complication arises from the uncertainty concerning the physical characterization of the oxide.

There have been many attempts to determine the coefficient of diffusion of oxygen in ZrO_2 . One method involves ^{18}O exchange between isotope enriched oxygen and microspheres of ZrO_2 which had been equilibrated at some predetermined oxygen pressure (14,15,16). Another method involves calculating the diffusion coefficient from electrical conductivity data by means of the Nernst-Einstein equation (16). The results from these analysis have good correspondence to a model based on an anti-Frenkle defect structure involving anion vacancies and interstitial anions (3,16). However, it is questionable whether the physical characteristics of the oxides studied are similar to the surface oxide that develops on bulk Zr. It has been demonstrated that the oxide produced on the metal surface has variable physical characteristics depending on temperature, oxidizing agent and environment, impurities in the Zr, and time of exposure to a specific environment.

Surface Science

The advent of surface sensitive spectroscopy methods has brought new direction to the study of the oxide development on Zr. There are many surface spectroscopy methods, including Auger electron spectroscopy (AES) and scanning electron microscopy (SEM) which have been used for Zr oxidation research.

For this work, SEM is used to develop morphological information. The physical characteristics of the surface oxides developed are compared to those found in the literature.

There has been little AES work on the surface oxidation of Zr reported in the literature. One method of AES analysis is associated with depth profiling. Another study technique involves oxidizing the Zr surface by exposing the surface to small amounts of O_2 . From these investigations, three regions of surface oxidation have been observed (17-20). The three regions of initial oxidation all lay within the first two regions shown in Figure 2. They are usually described as the chemisorption range, oxide nucleation range, and oxide thickening range. Samples of Zr have also been lightly oxidized while the sample is resistively heated (19,20,21). However, problems of diffusion of the oxygen into the bulk Zr has made it difficult to observe surface oxidation rates at high temperatures.

In this research, elemental Zr samples are oxygen saturated to form Zr:Oss. The Zr:Oss samples are utilized in an AES study of its surface properties and initial oxidation characteristics. A primary thrust of this investigation is to compare the initial oxide formation on Zr:Oss with that on pure Zr. Future work will involve kinetic studies of surface reactions on an oxide layer formed on the Zr:Oss samples prepared in this work.

RESEARCH OBJECTIVES

The overall goal is to investigate the simultaneous surface oxidation and absorption of oxygen into bulk Zr. Also, develop a method to produce oxygen saturated bulk Zr. The specific objectives were:

1. Prepare a mathematical model of the oxidation process. The model's principle parameters are diffusion coefficients of oxygen in Zr and ZrO_2 and the change in concentration of oxygen through the surface oxide layer.
2. Calibrate the model using experimentally determined values of oxide thickness and mass gain.
3. Prepare Zr:Oss samples.
4. Develop evidence confirming the saturation of the bulk Zr samples by AES depth profiling.
5. Observe the initial oxidation characteristics of Zr:Oss samples by AES and compare the results with the oxidation characteristics of pure Zr.

MODEL DEVELOPMENT

Mechanisms During Surface Oxidation of Zr

There are several physical processes that occur during the oxidation of Zr. These are diagrammed in Figure 3. The entire process can be broken down into several stages. If the rate controlling mechanism is determined and understood, a mathematical representation of the oxidation process may possibly be developed. There are four steps to the oxidation of Zr. First, oxygen must be adsorbed onto the oxide layer where it reacts to form O^{2-} ions. Second, the O^{2-} ions are transported through the oxide layer to the oxide metal interface. Third, the O^{2-} ions react with Zr to form ZrO_2 . Fourth, oxygen diffuses into the bulk metal.

The mechanisms involved with each step must be understood in order to model the oxidation process. It has been shown that the adsorption of oxygen onto the oxide surface is not rate limiting (3). There have also been studies on the diffusion of oxygen into bulk Zr, and the results appear to be consistent since various studies have determined similar diffusion coefficients, as mentioned previously.

The diffusion of oxygen through the surface oxide is assumed the rate limiting step during surface oxidation of

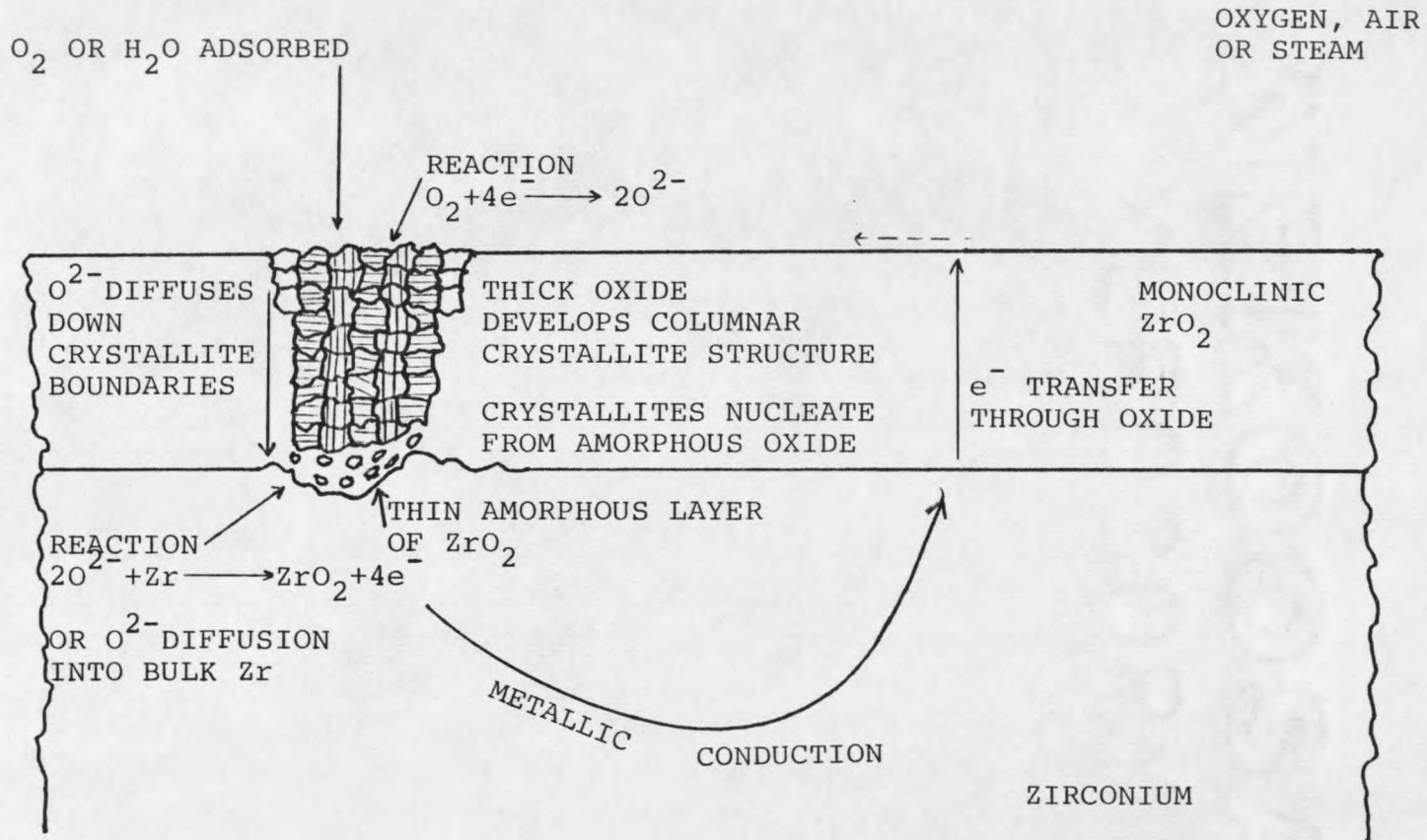


Figure 3. Schematic diagram of surface oxidation on Zr and the processes occurring in the oxide during oxidation.

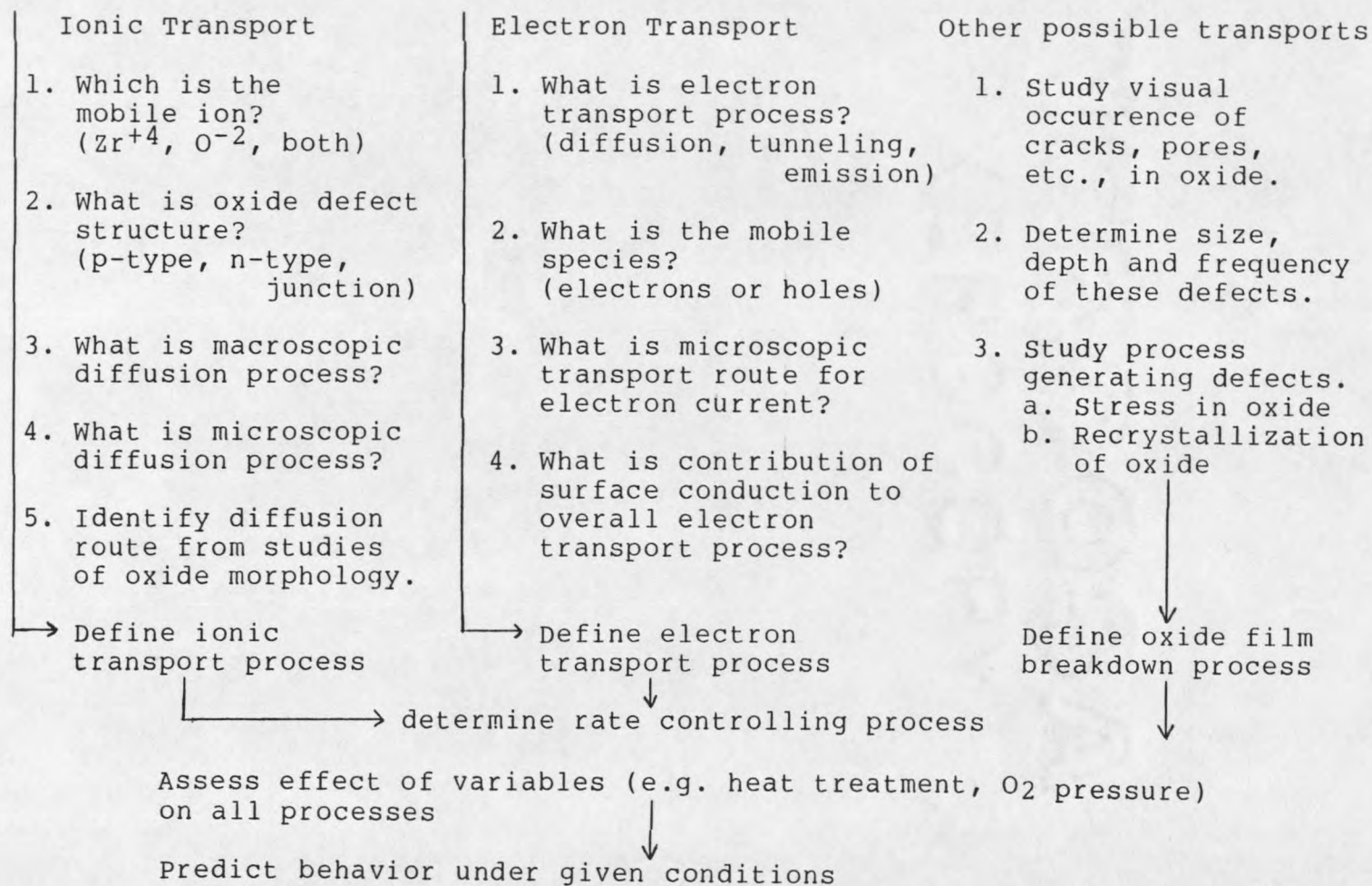
Zr. There are several possible mechanisms for the transport of oxygen through the oxide. Shown in Figure 4 is a list of the important mechanisms that may be involved in the surface oxidation of Zr (3). Figure 4 also suggests procedures for investigating each mechanism. The following is a discussion of the steps outlined in Figure 4, and an interpretation of their importance in developing a satisfactory model.

Ionic Transport in the Oxide

Throughout this analysis, O^{2-} ions have been referred to as the mobile species in the surface oxide. Although, Zr^{+4} could be the mobile ion, studies using injected rare gas atoms have shown that O^{2-} ions are most probably the mobile species (3). Studies of anodic films have shown that movement of Zr^{+4} ions represents less than 1% of the total ion transport (23):

Knowledge of the defect structure assists in the understanding of the method of movement of the mobile O^{2-} species. It has been demonstrated that the defect structure is p-type at pressures near atmospheric, and n-type at pressures below about 10^{-6} atm (24,25). However, these tests were performed on stabilized ZrO_2 samples. It is not clear whether the results apply to thin oxides grown on bulk Zr. There have been many attempts to determine the macroscopic diffusion coefficient of oxygen in ZrO_2 . The most popular and accurate methods involve nuclear reaction of oxygen (22) and $^{16}O/^{18}O$ exchange (26). These methods have been employed

Figure 4. Mechanisms that occur in the surface oxide during the oxidation of Zr.



on a growing oxide on bulk Zr. This eliminates the assumptions about the oxide's physical characteristics that must be made when using pure single crystals and polycrystalline spheres of ZrO_2 . There is about a 10^4 order of magnitude increase in the diffusion coefficients found for surface oxides over that of specially prepared bulk ZrO_2 .

Studies using ion bombardment mass spectrometry have determined that boundary diffusion of O^{2-} in polycrystalline ZrO_2 is a more important transfer method than lattice diffusion (27). The diffusion coefficients determined by the model in the following analysis takes into account both boundary and lattice diffusion. Their combined effect can be described as the effective diffusion coefficient.

An explanation for the second shift in the oxidation rate has been proposed based on the studies of diffusion paths (3). After nucleation and initial oxide growth, the grain boundary size of the oxide crystallites grow by continual recrystallization. At the start of oxidation, up to an oxide thickness of less than 200 \AA , the oxide consists primarily of an amorphous oxide structure (3). Further oxide growth involves the increase in size of the oxide crystals. When the oxide is 1000 to 2000 \AA thick, the crystallites displace the amorphous oxide and occupy 100% of the surface (17-20). As size of the crystallite increases, the area available for boundary diffusion decreases.

